Applied Catalysis B: Environmental 132–133 (2013) 62–69

Contents lists available at SciVerse ScienceDirect

Applied Catalysis B: Environmental

journal homepage: www.elsevier.com/locate/apcatb

Mixed metal nanoparticles loaded catalytic polymer membrane for solvent free selective oxidation of benzyl alcohol to benzaldehyde in a reactor

S. Prakash, Chumki Charan, Ajay K. Singh, Vinod K. Shahi*

Electro-Membrane Processes Division, Central Salt and Marine Chemicals Research Institute, Council of Scientific & Industrial Research (CSIR), G.B. Marg, Bhavnagar-364002, Gujarat, India

ARTICLE INFO

Article history:
Received 15 August 2012
Received in revised form 1 October 2012
Accepted 1 November 2012
Available online 24 November 2012

Keywords:
Selective oxidation
Catalytic polymeric membranes
Catalytic membrane reactor
Metal nanoparticles, Solvent free reaction

ABSTRACT

Catalytic polymer membrane (CPM) was prepared by *in situ* loading of mixed (silver and lead) metal nanoparticles (MNPs) in sulfonated poly(ether sulfone) (SPES) matrix. Developed membrane (SPES-Ag^0(35)/Pb^0(65)) was used as a catalyst (oxidant) loaded and separator, in two-compartment catalytic membrane reactor (CMR) for selective oxidation of benzyl alcohol (BnOH) to benzaldehyde (BzH) in ambient conditions without regeneration of catalysts, separation steps and waste generation. CPM acts as barrier and contactor between organic and aqueous phase, which was characterized by FTIR, XRD EDX, SEM, and physicochemical properties. Reported SPES-Ag^0(35)/Pb^0(65) showed good solvent, chemical and thermal stabilities in compare with fluorinated membrane and assessed to be more suitable for CMR. Effects of various reaction parameters such as substituted BnOH, concentration, silver nanoparticles (AgNPs) load *etc.* were investigated. High performance, low cost and stability of reported SPES-Ag^0(35)/Pb^0(65) suggested its commercial viability for chemical transformations in CMR.

1. Introduction

Generally, oxidation of hydrocarbons has been achieved by heavy metal reagents and toxic solvents, which generates hazardous waste. Based on principle of green chemistry, selective oxidation of hydrocarbons is an important chemical transformation. Aldehydes and ketones are essential chemicals, synthesized by oxidation of alcohols in presence of volatile organic solvents using stoichiometric inorganic oxidants, and chromium reagents [1–4]. From point view of green chemistry, there is an exigent demand for efficient, cost-effective and environmentally benign process for synthesis of aldehydes and ketones, which avoids catalyst recycling, clean oxidants such as O_2 [1,5–10].

CMR offers many practical advantages and considered as an innovative device for achieve the chemical transformations with high selectivity, without any additional costs of separation of by-products and waste generations. CMR with hydrophobic/hydrophilic CPMs were highly desirable during catalytic chemical and biochemical reactions [11–15]. To enhance the interfacial area of metal catalysts in CPMs, immobilization of metal nanoparticles (MNPs) attracted increasing attentions due to high percentage of surface atoms and the associated quantum effects [16,17]. To avoid the MNPs aggregation and enhance their stabilization without any catalyst loss or recovery, incorporation of MNPs in polymer matrix offers unique possibilities for enhanced access of reactants to the catalytic sites [18,19]. *In situ* synthesis of MNPs into a polymer matrix permits synergised catalytic activity, without any destruction and pollutants separation [20,21]. Thus, CPMs should consists of stable (chemical, thermal, and mechanical), and processable polymer matrix [22].

Numerous polymeric membranes such as PVDF [23,24], PTFE [25], alumina [26], lead Nafion® 417 coated ruthenate pyrochlore [27], PDMS/PVA [11], Fenton coated Nafion [28] and ceramics [29], were used in CMR., because of their excellent stabilities in harassed conditions [17–19]. But, hydrophilic/hydrophobic modifications of these polymeric membranes are difficult. As an alternate, poly (ether sulfone) (PES) were successfully proposed as cost effective, fluorine-free polymer [30–32]. PES is a moderate oxidative, solvent resistance and stable (mechanical, chemical and thermal) polymer, because of aromatic rings and strong chemical bonding between carbon, sulfur and oxygen [32–35]. Further, functionalization (sulfonation) of PES provides acidic membrane matrix, suitable for loading of metal ions by ion-exchange and further metal ions reduced by strong reducing agent to MNPs formation. This novel approach for developing MNPs loaded CPMs completely ruled out the leaching of catalytic active centre. Thus, suitability of MNPs loaded SPES membrane has explored as CPM (SPES-Ag^0(35)/Pb^0(65)) for selective oxidation of benzyl alcohol (BnOH) to benzaldehyde (BzH) in a CMR.

Selective oxidation of BnOH to BzH is of industrial importance, use of latter in cosmetics and flavour industries, in which presence of impurities (organic chlorine or benzoic acid) is a serious

* Corresponding author. Tel.: +91 9925125760; fax: +91 278 2567562/6970.
E-mail addresses: vkshahi@csmcri.org, vinodshahi1@yahoo.com (V.K. Shahi).

0926-3373/$ – see front matter © 2012 Elsevier B.V. All rights reserved.
http://dx.doi.org/10.1016/j.apcatb.2012.11.001

concern [36,37]. Furthermore, the present route does not conform the guidelines of green chemistry (zero discharge, maximum atom utilization efficiency, avoid the use of solvents, and catalysts) [15]. High performance catalysts with low temperature activity/selectivity are also challenge. Silver based catalysts including electrolytic silver catalyst has been reported for gas phase selective oxidation of BnOH to BzH [38]. But electrolytic silver is not active below 500 °C and not selective above 500 °C because of cracking and over oxidation [38]. Recently supported silver catalyst on Ni-fibers has been demonstrated for gas phase selective oxidation of BnOH to BzH with 91% conversion and about 85% selectivity at 380 °C [10]. Latter on same research group also proposed Ag/Ni fiber catalysts for the selective oxidation of BnOH at 120 °C. But regeneration of catalysts, separation of un-reacted reactants and products and reaction at elevated temperature, are unsolved limitations.

Herein, we are reporting highly selective and stable CPMs loaded with MNPs (Ag^o and Pb^o) in the acidic functionalized SPES matrix for selective oxidation of BnOH to BzH without any by-product or waste generation and separation steps in a CMR. Reported process showed selective oxidation at the interface of CPM, and due to low permeation of BzH across the CPM to aqueous phase, its over-oxidation was protected.

2. Experimental

2.1. Materials

PES (Udel P-3500) was received from Solvay Advanced Polymers. Benzyl alcohol (BnOH), p-anisyl alcohol, m-nitro benzyl alcohol, methanol, toluene, silver nitrate, lead nitrate, hydrazine hydrate of AR grade, were obtained from S.d fine Chemicals, India. All chemicals were used without any further purification. Double distilled water was used for all experiments.

2.2. Preparation of catalytic polymeric membrane

Detailed procedures for sulfonation of PES and preparation of SPES membranes have been described (Section S1, Supporting informations) [34]. SPES membranes were conditioned in HCl and NaOH solutions (0.10 M) alternatively, and washed with distilled water. Procedures for estimation of water content, ion-exchange capacity (IEC), membrane tortuosity (τ) and porosity (ε) are included (Section S2, Supporting informations). Physicochemical and electrochemical properties of SPES membranes are included in Table S1 (Supporting informations). Thickness of the membrane was measured as average values of three consecutive measurements with digital micrometer (1.0 μm sensitivity).

Fig. 1 shows the typical preparation methodology for the catalytic polymeric membrane (CPM). A piece of SPES membrane (25 cm^2) was equilibrated with mixed solution (35 mM $AgNO_3$ and 65 mM $PbNO_3$) to allow the exchange of H^+ with Ag^+ or Pb^{2+} for 24 h. After careful washing with deionised water, membrane was immersed in hydrazine hydrate (1.75 wt%) at 50 °C for 24 h, to reduce the metal ions into metal nanoparticles (MNPs). Three CPMs (SPES-Ag^0(35)/Pb^0(65); SPES-Ag^0(50)/Pb^0(65)and SPES-Ag^0(65)/Pb^0(65)) were prepared in which loading Pb^0 NPs was constant (65 mM $PbNO_3$) while loading of Ag^0 NPs was varied (35–65 mM $AgNO_3$) in the SPES matrix.

Uniform distribution of MNPs (catalytic active sites) on the membrane surface was confirmed by SEM images. Loading of MNPs in the membrane phase was obtained from weight difference method and varied between 60 and 75 mg/g (0.25–0.40 mmol of metal ions per gram of dry weight membrane). Photo images of the SPES and SPES-Ag^0(35)/Pb^0(65)membranes are depicted in Fig. S1 (Supporting informations), which also confirmed loading of MNPs in the SPES matrix.

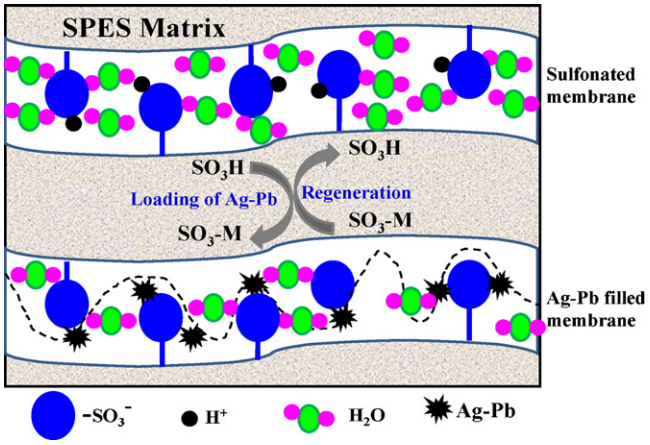

Fig. 1. Schematic presentation of CPM used in CMR.

2.3. Mass transport model

When reactants contact by diffusion across the SPES-Ag^0(35–65)/Pb^0(65) matrix, the chemical conversion strongly influenced by the catalytic performance of diffusing medium (Fig. S2, Supporting informations). For best performance, mass transfer resistance should be low with limited reaction regime. Prepared SPES-Ag^0(35–65)/Pb^0(65) membranes were nanoporous with 29–20% overall porosity (ε) (Table 1). Diffusivity (D_{eff}) across SPES-Ag^0(35–65)/Pb^0(65) membrane differs from the bulk (D_0) and its values can be determined by overall porosity (ε), and tortuosity (τ), which revealed the membrane porous structure and steric hindrance:

$$D_{eff} = \frac{D_0 \varepsilon}{\tau \theta} \quad (1)$$

where,

$$\theta = \left[\frac{r_p - r_s}{r_p}\right]^4 \quad (2)$$

r_p is mean radius of the pore, while r_s 'Stokes radius of the reagent' can be obtained by [23].

$$r_s = \frac{\kappa_B T}{6\pi\eta D} \quad (3)$$

k_B is the Boltzmann constant ($J\,K^{-1}$), D is the diffusion coefficient ($m^2\,s^{-1}$), η viscosity of solution and T is the absolute temperature.

2.4. Instrumental analysis and membrane stabilities

Detailed instrumental analysis have been included in the section S3 (supporting informations). Oxidative stability of SPES-Ag^0(35–65)/Pb^0(65) membranes was evaluated in Fenton's reagent (3% H_2O_2 aqueous solution containing 3 ppm $FeSO_4$) at 80 °C for 1 h. For the hydrolytic stability test, a small piece of membrane (30 mm) was boiled in water for 24 h at 100 °C in a pressurized closed vial. Membrane stability was evaluated in turns of weight loss and the physical appearance of the test samples. Chlorine stability tests were assessed in 5% NaOCl aqueous solution at 80 °C for different

Table 1
Physicochemical properties for SPES and different CPMs membranes.

Membrane	φ_w (%)	t (μm)	τ	θ	ε	ε/τ
SPES	13.7	150	0.93	0.34	0.39	0.42
SPES-Ag^0(35)/Pb^0(65)	5.80	127	0.85	0.29	0.22	0.25
SPES-Ag^0(50)/Pb^0(65)	4.10	135	0.80	0.24	0.29	0.36
SPES-Ag^0(65)/Pb^0(65)	2.89	137	0.74	0.25	0.20	0.27

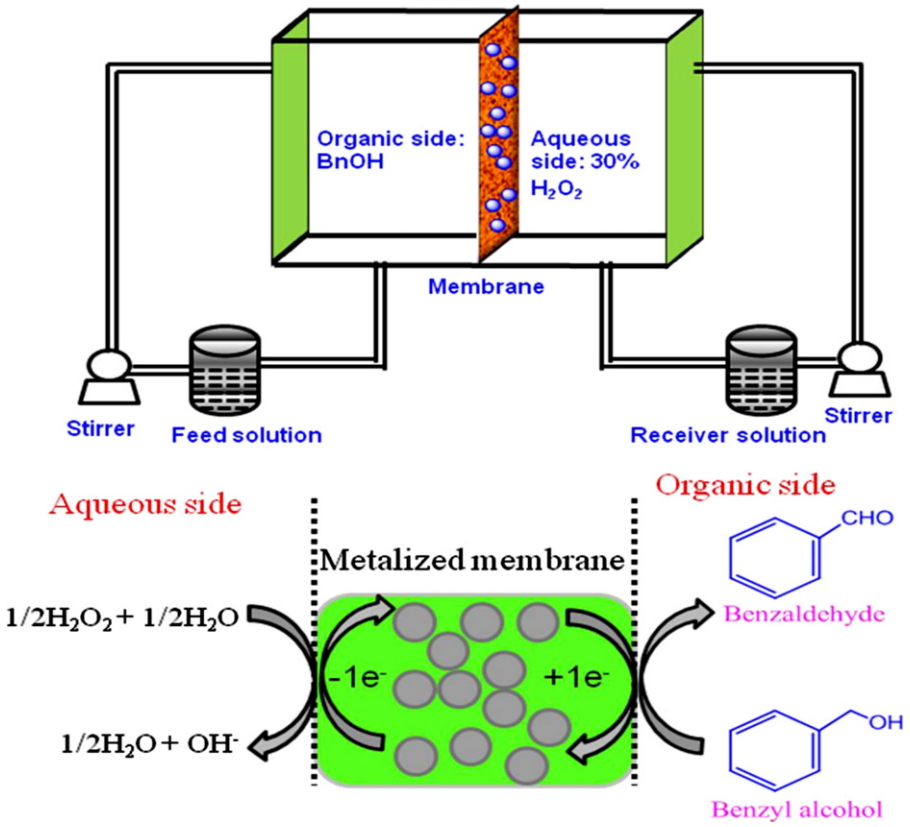

Fig. 2. Schematic representation of CMR.

interval times [39,40]. Dimensional stability was examined in water at room temperature for 24 h [41].

2.5. Oxidation of benzyl alcohol in CMR

Experiments were performed in a specially designed two-compartments CMR (50.0 cm^3), separated by SPES-Ag^0(35–65)/Pb^0(65) membranes (25 cm^2) with 2.4 mg cm^{-2} MNP loaded (Fig. 2). H_2O_2 solution (30%; 50 cm^3) and benzyl alcohol (BnOH) (5 mmol; 50 cm^3) solution were recirculated through aqueous and organic phase, respectively. Reaction temperature was constant (70 °C) with 1.5 cm^3/min feed flow rate of each stream by two peristaltic pumps. Samples were periodically analysed by GC-MS and NMR. For NMR analysis, $CDCl_3$ (deuteron chloroform) was used as solvent for benzaldehyde (product).

3. Results and discussion

3.1. Characterizations of SPES-MNPs membranes

Degree of sulphonation (DS) for PES (62.0%) was evaluated by ^{1}H-NMR spectra (Fig. S3 (supporting informations)) [34]. It is important to record that SPES with high degree on sulphonation (< 65%) forms unstable water adduct. Thus, optimization of DS is necessary for membrane stability. FTIR spectra of SPES (Fig. S4, Supporting informations) showed peak at 1030 cm^{-1} due to symmetric stretching of S=O for conformed -SO_3H groups into the polymer matrix. Similar spectrum was also obtained for SPES-Ag^0(35)/Pb^0(65) membrane. XRD patterns of Ag/Pb NPs, SPES and SPES-Ag^0(35–65)/Pb^0(65) membranes were included in Fig. 3. Ag/Pb NPs exhibited a broad 2θ peak centred at 37.7° and another diffuse wave in the window of 40–80°. XRD patterns for SPES-Ag^0(35–65)/Pb^0(65) membranes showed sharp peaks at 37.7, 43.9, 64.0 and 77.0° (standard values of the Ag/Pb crystalline powder) [42]. Further, XRD peaks for SPES-Ag^0(35–65)/Pb^0(65) membranes were relatively sharper in comparison to Ag/Pb NPs, which confirmed crystallization of Ag/Pb in SPES interfacial structures.

The peak broadening may be related to strain, faulting, and grain size in XRD patterns, [43,44]. The strain and faulting can be easily predicted by 2θ-peak shift. For all three cases virtually the same major peak (2θ =37.7°) ruled out the possibility of strains and faulting. The grain size (d, nm) change caused peak broadening, and for Ag/Pb NPs can be calculated from the broadening of XRD peak using the Debye-Scherrer formula below [43].

$$d = \frac{\kappa\lambda}{\beta\cos\theta} \quad (4)$$

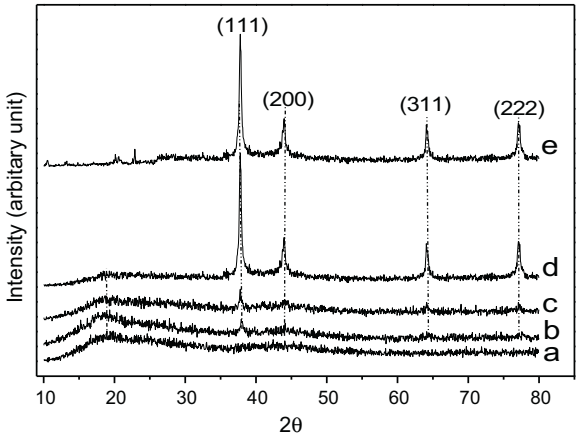

Fig. 3. XRD of: (a) SPES, (b) SPES-Ag^0(35)/Pb^0(65); (c) SPES-Ag^0(50)/Pb^0(65); (d) SPES-Ag^0(65)/Pb^0(65); and (e) Ag^0(35)/Pb^0(65) powder sample.

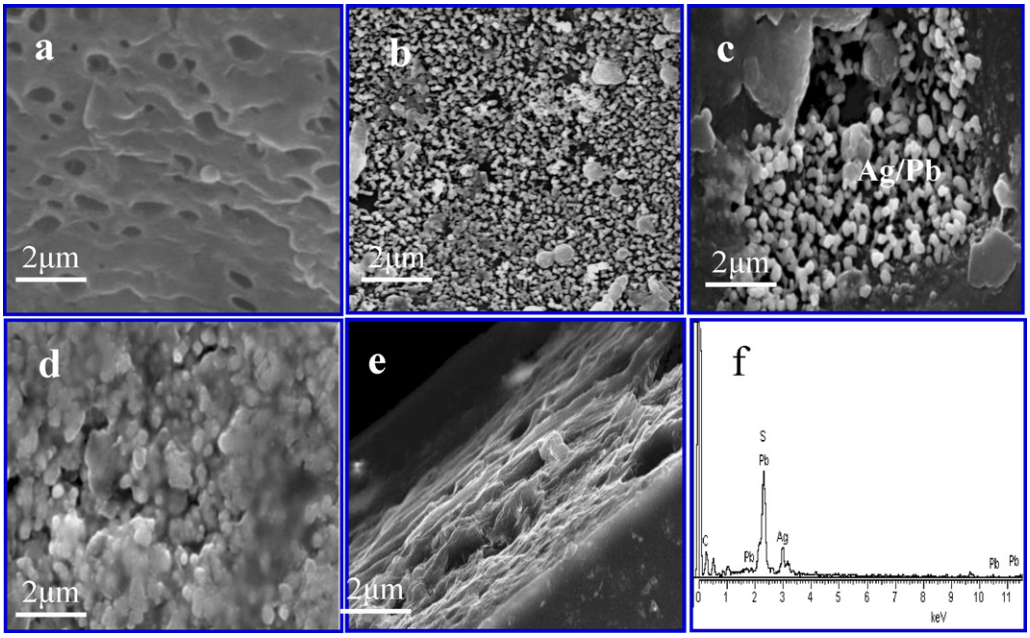

Fig. 4. SEM of: (a) porous SPES, (b) SPES-Ag^0(35)/Pb^0(65); (c) SPES-Ag^0(50)/Pb^0(65); (d) SPES-Ag^0(65)/Pb^0(65) membrane; (e) cross-sectional view of c; and (f) EDX of c.

where 'λ' is the X-ray wavelength (0.1542 nm), 'β' is the full width of the half maximum (FWHM) value (in radians), and 'κ'shape factor (0.8–1.2). Peak at 2θ =37.7° was taken uniformly for the "d" assignment. An FWHM value of 0.246° was calculated for the SPES-NPs membrane [45]. For the Ag-Pb NPs and SPES-Ag^0(35–65)/Pb^0(65) samples, "d" values were estimated about 85.6 and 20.2 nm, respectively. The crystalline grain size of Ag-Pb NPs was about four times as large in compare with SPES-Ag^0(35–65)/Pb^0(65), which was related to the membrane structural factor.

SEM images and energy dispersive X-ray analysis (EDX) of SPES-Ag^0(35–65)/Pb^0(65) membranes (Fig. 4) showed nano-spherical surface morphology without any marked cracks. Size of Ag NPs was about 50 nm, while Pb NPs showed large nano-cluster (particle size ~ 800 nm). Isolated and uniformly distributed Ag-Pb NPs (5.3 nm) in SPES-Ag^0(35–65)/Pb^0(65) membranes were observed similar to TiO_2 modified Nafion® membrane [46]. Membrane cross-section was unaltered significantly after MNPs loaded. SPES have rigid and stable network with hydrophilic channels, which rugged enough to protect the network from surface cracks even in harsh environments.

Table 1 showed physicochemical properties (thicknesses, pore size and porosity) for SPES and different SPES-Ag^0(35–65)/Pb^0(65) membranes. Membrane porosity decreased with increase in MNPs loaded may be due to blockage of pore channels. This observation was also supported by SEM images. φ_w value for SPES membrane (13.7%) was reduced to (2–5%) after MNPs loaded (Table 1). These observations imply that: (i) hydrophilic membrane forming material does not result membrane dissolution, and (ii) loading of Ag-Pb NPs does not substantially affected the membrane morphology and water accessibility to the sulfonic acid groups.

Porosity of SPES-Ag^0(35–65)/Pb^0(65) membranes plays a crucial role during the diffusion of BnOH, and diffusivity (D_{eff}) was governed by pore size (r_p), porosity (ε), and tortuosity (τ). In particular, D_{eff} increased with θ value and was inversely proportional to τ. SPES-Ag^0(35–65)/Pb^0(65) membranes showed equal θ values and different ε/τ values. SPES-Ag^0(65)/Pb^0(65) membrane showed lowest ε/τ value (0.27) due to low diffusivity.

Cation-exchange nature of the membrane was evaluated by ion-exchange capacity (IEC) measurements using acid-base titration [40,41]. SPES membrane showed 1.20 mequiv./g IEC, while SPES-Ag^0(35–65)/Pb^0(65) membranes did not show any IEC may be due to blocking of exchangeable sites by MNPs.

3.2. Thermal, oxidative, hydrolytic, chlorine and solvent stabilities

TGA curves of SPES and SPES-Ag^0(35–65)/Pb^0(65) membranes (Fig. 5) showed three weight loss stages. Initial weight loss (50–127 °C) aroused due to desorption of water from the membrane matrix, while second weight loss (170– 450 °C) assigned to desulfonation of membrane matrix. Fascinatingly, SPES-Ag^0(35–65)/Pb^0(65) possessed low weight loss in compare with pristine membrane (SPES) because of loading of MNPs. Third weight loss (450–650 °C) ascribed to polymer degradation. Thus, below 400 °C the rigid and stable SPES-Ag^0(35–65)/Pb^0(65) membranes was suitable for CMR.

Hydrogen peroxide and hypochlorite are useful catalysts for synthesis of BzH [40,41], thus CPM (SPES-Ag^0(35)/Pb^0(65)) should be highly stable in strong oxidative environment. The oxidative stability of SPES-Ag^0(35)/Pb^0(65) membrane was assessed compared with SPES and Nafion 117 membrane in Fenton's reagent (3% aq.

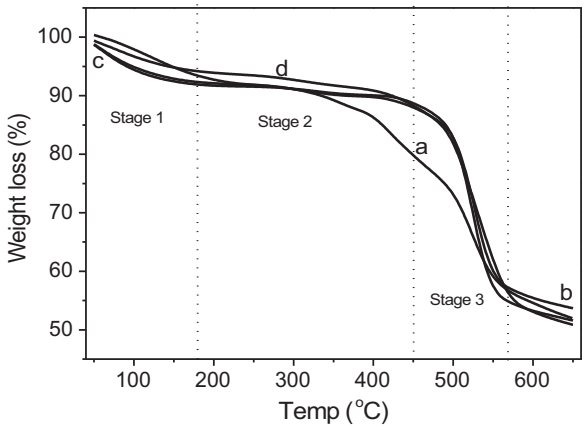

Fig. 5. TGA curves for: (a) SPES, (b) SPES-Ag^0(35)/Pb^0(65); (c) SPES-Ag^0(50)/Pb^0(65); and (d) SPES-Ag^0(65)/Pb^0(65) membranes.

H_2O_2 + 3 ppm $FeSO_4$) in terms of weight loss (Fig. S5A, Supporting informations). Both membranes (SPES-Ag^0(35)/Pb^0(65) and Nafion 117) showed negligible weight loss about (1.0–1.2%). The membrane degradation occurs as result of the $^{\bullet}OH$ and $^{\bullet}OOH$ radicals, which attack on the polymeric back bone locality of the hydrophilic group. SPES-Ag^0(35)/Pb^0(65) membrane exhibited comparable oxidative stability to Nafion-117 membrane because of hydrophilic groups (-SO_3H) the membrane matrix surrounded by metallic cluster. Membrane boiling water (hydrolytic) test was also performed for 24 h, which showed good stability. Also, SPES-Ag^0(35)/Pb^0(65) membrane was highly stable in acid environment (8.0 M HCl) with 1–3% swelling.

Chlorine tolerant nature of SPES-Ag^0(35)/Pb^0(65) membrane was assessed in compare with pristine SPES and Nafion 117 membrane by recording weight loss in NaOCl environment (oxidizing agent) [24]. SPES-Ag^0(35)/Pb^0(65) membrane showed 5–7% weight loss after 20 h treatment (Fig. S5B, Supporting informations). The membrane degradation occurs due to attack of oxy-chloride free radical in the vicinity of hydrophilic domains [40,41], which was surrounded by MNPs clusters in case of SPES-Ag^0(35)/Pb^0(65) membrane. Furthermore, these membranes are stable in chlorine environment.

To assess the suitability of CPM for CMR, solvent stability membranes are an important parameter. SPES-Ag^0(35)/Pb^0(65) membrane showed no significant weight loss (%) and morphology changes (Table S2, Supporting informations) under different solvents (methanol, benzene, toluene, cyclohexane, cyclohexanol, trichloroethane, and petroleum ether) even after 72 hours. In case of polar solvents (acetone, dioxane, chloroform, dichloromethane, cyclohexanone, trichloroethylene), SPES-Ag^0(35)/Pb^0(65) membrane was unstable and turned brittle.

3.3. Selective oxidation of benzyl alcohol to benzaldehyde

The catalytic oxidation of BnOH was carried out in a CMR made of Teflon material and containing two chambers (aqueous and organic) separated by SPES-Ag^0(35–65)/Pb^0(65). Aqueous chamber was recirculated by co-oxidant (H_2O_2 solution), while organic chamber was recirculated with BnOH. SPES-NPs membrane was placed in such way that MNPs loaded surface faced aqueous phase. Flow rate of the both streams was kept constant (1.0 cm^3/min). Reaction rate were continuously monitored by GLC and ^{1}HNMR) at different interval time (Fig. S6, Supporting informations). The influence of several parameters (BnOH concentration, solvent, substituted group, temperature and flow rate) was investigated to optimise the process performance and to avoid the further oxidation of the BzH to benzoic acid.

Conversion (%), selectivity (%) and yield (%) to benzaldehyde were estimated by following eq.5 and 6.

$$Conversion(\%) = \frac{A}{A_i} \times 100 \quad (5)$$

$$Selectivity(\%) = \frac{A}{A+B} \times 100 \quad (6)$$

$$Yield(\%) = Conversion \times Selectivity \times 100 \quad (7)$$

where A and B are concentration (mmol) of benzyl alcohol and benzaldehyde, respectively. A_i is initial concentration of benzyl alcohol. Silver redox couple participated in the oxidation of benzyl alcohol in the presence of H_2O_2 (Fig. 2) [47–49]. In the first step, co-oxidant H_2O_2 oxidized Ag^0 to Ag^+ in aqueous solution, which in turn oxidized the benzyl alcohol to benzaldehyde (organic phase) and further attained Ag^0 state in cyclic manner (Fig. 2). Electrogeneration of silver ion intermediate is an important aspect during oxidation of benzyl alcohol [47–49]. H_2O_2 acts as sacrificial electron acceptor during overall oxidation. It was expected that cationic sites of the membrane matrix easily abstract the proton from BnOH [48].

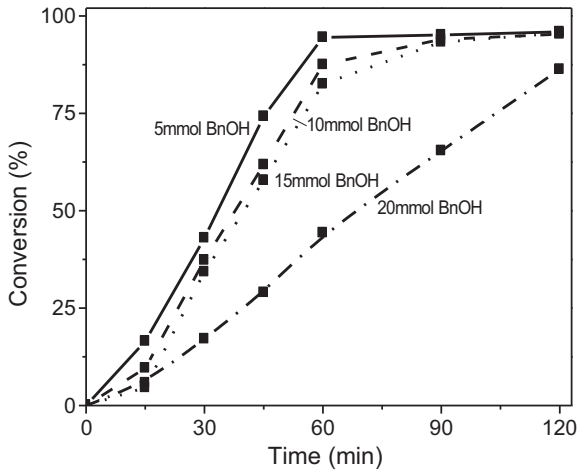

Fig. 6. Variation of conversion rate with time during oxidation of BnOH (different concentration) to BzH under optimum conditions in CMR.

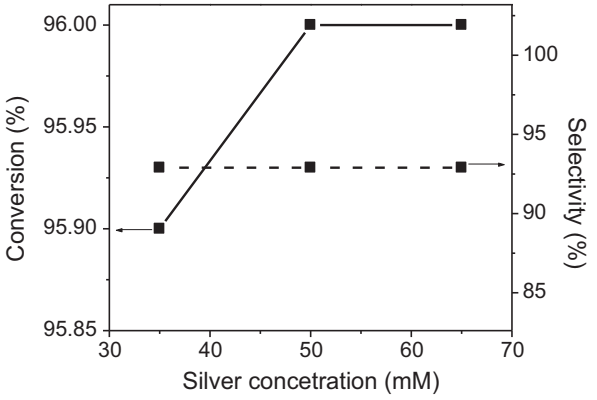

Fig. 7. Effect of Ag NP loading on conversion rate and selectivity for oxidation of BnOH to BzH under optimum conditions in CMR.

Reactant concentrations affect the reaction rates (Fig. 6), and conversion rate increased with BnOH concentration. At low BnOH concentration (5 mmol), selectivity was 92%, while it was decreased to 86.3% for 20 mmol. Thus conversion rate depends on the reactant concentration. A series of substituted benzyl alcohols were selectively oxidized under optimised system conditions (Table 2). Presence of an electron-withdrawing substituent on the benzene ring enhanced reaction time with reduced product yield.

Loading of metal catalyst in the membrane matrix also affects the conversion rate (Fig. 7). With constant Pb NPs loaded, conversion rate increased slightly with increase in loading of Ag NPs, because of catalytically active nature of Ag^+. Close to 96.0% conversion with 92.3% selectivity was obtained, with optimum loading of MNPs. Concentration of H_2O_2 (co-catalyst) showed small effect on

Table 2
Oxidation of substituted benzyl alcohols to aldehydes using CPM under optimum conditions.[a]

Substrate	Yield (%)[b]	Selectivity (%)
p-Methoxy benzyl alcohol	73.0	83
p-Nitro benzyl alcohol	61.0	79
Benzyl alcohol	95.9	92

[a] Reaction conditions: substrate (5 mmol), aqueous solution of 30% H_2O_2 (25 ml) and SPES-Ag^0(35)/Pb^0(65) membrane at 27 °C.
[b] By quantitative NMR.

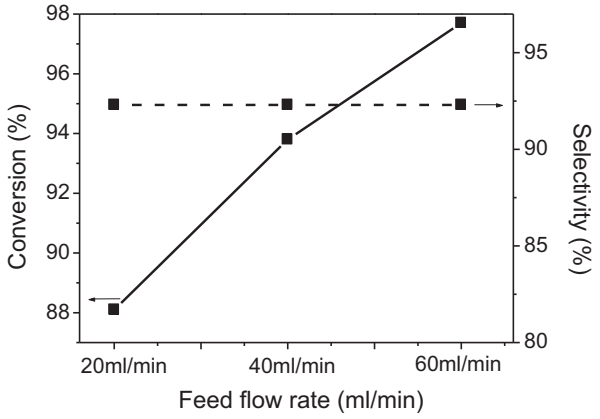

Fig. 8. Effect of flow rate of organic stream on conversion rate and selectivity for oxidation of BnOH to BzH under optimum conditions in CMR.

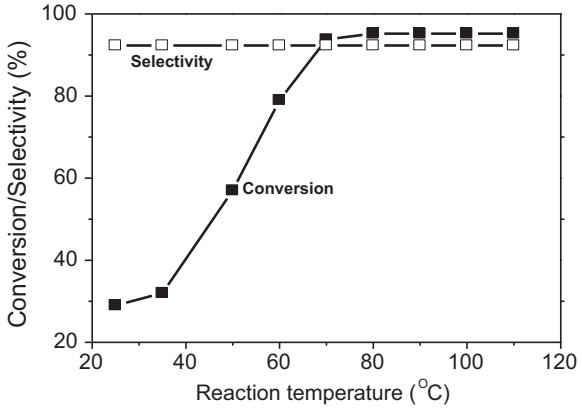

Fig. 9. Effect of temperature on conversion rate and selectivity for oxidation of BnOH to BzH under optimum conditions in CMR.

the conversion rate, while it strongly influenced the selectivity of the reaction.

Feed flow rate or turbulence also affects the rate of oxidation reaction. Conversion rate of BnOH to BzH, increased from 88.1% to 97.7% with increase in flow rate of organic phase (20–40 cm^3/min) without any significant deterioration in reaction selectivity (92.3%), (Fig. 8). This observation was attributed to enhanced mass transfer at high flow rate. Malek et al. reported reduced mass-transfer rate at a high liquid velocity (flow rate), due to relatively greater potential of liquid to wet the catalytic membrane [50]. However, in this case, 60 cm^3/min feed flow rate of organic phase was optimized for high formation rate of BzH (Fig. 8) [50].

3.4. Effect of temperature and kinetic study

Conversion rate of BnOH increased with reaction temperature (25–110 °C) (Fig. 9), without any alteration in selectivity. The rate constants were calculated by pseudo-first order kinetic models [40]:

$$\log(C_e - C_t) = \log C_e - \frac{k_1 t}{2.303}$$

C_e and C_t are the benzaldehyde concentration at equilibrium and time t. Values of first order rate constant (k_1) (estimated by slope of $\log(C_e - C_t)$ *vs* t linear plots) (Fig. 10)) and correlation coefficient (R^2) confirmed pseudo first order kinetics of BnOH oxidation to BzH (Table 3).

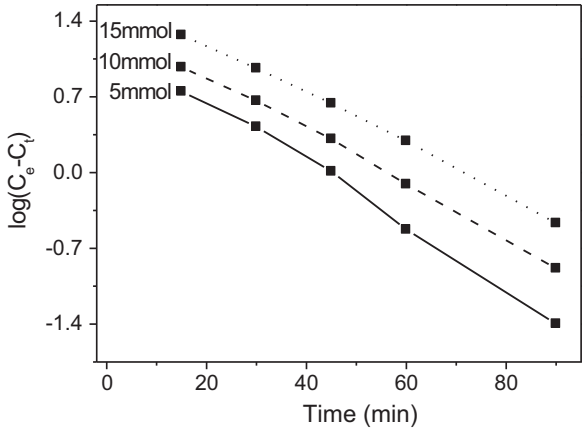

Fig. 10. Pseudo first order kinetics at carried BnOH concentration during its oxidation to BzH under optimum conditions in CMR.

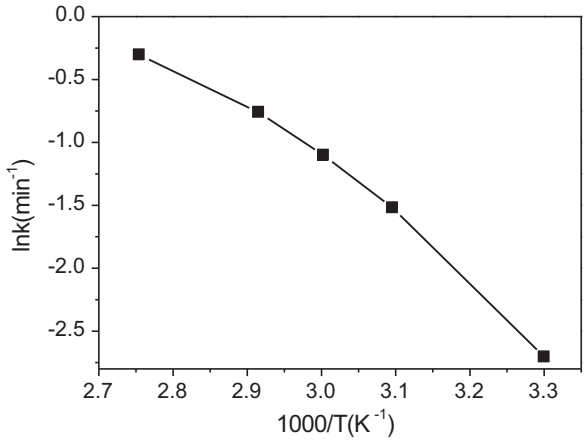

Fig. 11. Arrhenius plot for oxidation of BnOH to BzH under optimum conditions CMR.

The dependence of conversion rates on temperature manifests dependency of rate constant (k).

$$\ln k = \ln A - \frac{E_a}{RT} \quad (8)$$

where R is the universal gas constant (8.314 J mol^{-1} K^{-1}), A frequency factor, E_a activation energy, and T the absolute temperature (K). 6.815 kJ.mol^{-1} of E_a value was obtained (Fig. 11). Mobility of molecules increases with temperature, which further leads increase in collision frequency and reaction rate.

3.5. Oxidation of other alcohols

Oxidation of BnOH was studied as a model reaction, but oxidation of other homologues alcohols (propanol, isopropanol, butanol,

Table 3
Pseudo-first order kinetics constants (k_1) and correlation coefficients (R^2) for oxidation process of benzyl alcohol.

Concentration (mmol)	Pseudo- first -order kinetics	
	K_1 (min^{-1})	R^2
5	0.066787	0.9970
10	0.057575	0.9979
15	0.052969	0.9957

Table 4
Oxidation of other homologous alcohols under optimum conditions.[a]

Substrate	Yield (%)[b]	Selectivity (%)
Propyl alcohol(PA)	81.1	78.2
Isopropyl alcohol(IPA)	20.3	79.4
Butanol(BA)	70.2	81.2
Isobutanol(IBA)	46.0	80.5
Amyl alcohol(AA)	72.0	77.3
Isoamyl alcohol(IAA)	35.1	72.1

[a] Reaction conditions: substrate (5 mmol), aqueous solution of 30% H_2O_2 (25 ml) and SPES-Ag^0(35)/Pb^0(65) membrane at 27 °C.
[b] By quantitative NMR.

isobutanol, amyl alcohol and isoamyl alcohol) was also studied in CMR (Table 4). Under similar conditions, comparatively lower oxidation reactivity for these primary alcohols was observed, which was attributed to their different aromatic structure. For the aliphatic secondary alcohols (isobutanol and isoamyl alcohol) low product yield (35.1–46.0%) was observed due to steric effect. It is worthy to note that oxidation of butanol, isobutanol, amyl alcohol and isoamyl alcohol approached to biphasic catalysis due to their less solubility in water. However, the systems of propanol and isopropanol oxidation exhibited characteristic of analogously homogeneous catalysis due to easy solubility of them and their reaction products in water. Thus, these catalytic systems showed relatively lower conversion rate in compare with oxidation of BnOH.

The catalyst recycling was also investigated up to ten cycles. No significant deterioration in catalyst activity was observed. Further, in long-term application, membrane catalytic activity may be restored by its washing in sequence with copious amount of toluene, acetone, and water (under stirred condition for 1 h in each case). Washed catalytic membrane was further dried at 50 °C for 3 h, to achieve ~100% catalytic activity.

4. Conclusions

A promising catalytic membrane reactor (CMR) containing Ag-Pb NPs loaded on SPES matrix) has been proposed for low temperature and selective oxidation of benzyl alcohol (BnOH) to benzaldehyde (BzH). Prepared CPM showed excellent thermal, solvent and oxidative stabilities under experimental conditions, which are the essential requirements for its applications in CMR. Most suitable SPES-Ag^0(35)/Pb^0(65) exhibited 92% selectivity and 95.9% conversion for oxidation of BnOH to BzH using CMR under optimum operating conditions. This method completely avoids regeneration of spent catalysts, separation un-reacted reactants and products and high conversion and selectivity were achieved at ambient temperature.

In compare with conventional method, CPM plays similar role to phase transfer catalyst, and acts as interphase contactor in a biphasic reaction. Thus, developed CMR is suitable for static and continuous production of benzaldehyde from BnOH. Further development is in progress to improve catalyst life-time and novel approach to engineer the MNPs-polymer interaction.

Acknowledgements

One of the authors S. Prakash is thankful to Council of Scientific and Industrial Research (CSIR), New Delhi, for providing Senior Research Fellowship (SRF). We are also very grateful to Mr. J.C. Chaudhari at CSMCRI (CSIR) for SEM measurements of the samples. We also acknowledge the services of analytical science division, CSMCRI, Bhavnagar for instrumental support

Appendix A. Supplementary data

Supplementary data associated with this article can be found, in the online version, at http://dx.doi.org/10.1016/j.apcatb.2012.11.001.

References

[1] T. Mallat, A. Baiker, Chemical Reviews 104 (2004) 3037–3058.
[2] J. Shen, W. Shan, Chemical Communications (2004) 2880–2881.
[3] R.P. Unnikrishnan, S.D. Endalkachew, Journal of Catalysis 211 (2002) 434–444.
[4] M. Hudlicky, Oxidation in Organic Chemistry, American Chemical Society, Washington, DC, 1990.
[5] G. Zhao, H. Hu, M. Deng, Y. Lu, Chemical Communications 47 (2011) 9642–9644.
[6] G. Zhao, H. Hu, M. Deng, Y. Lu, Chem. Cat. Chem. 3 (2011) 1629–1636.
[7] G. Zhao, H. Hu, M. Deng, M. Ling, Y. Lu, Green Chemistry 13 (2011) 55–58.
[8] J.P. Mao, M.M. Deng, L. Chen, Y. Liu, Y. Lu, AIChE Journal 56 (2010) 1545–1556.
[9] M. Deng, G. Zhao, Q. Xue, L. Chen, Y. Lu, Applied Catalysis B: Environmental 99 (2010) 222–228.
[10] M.J. Beier, B. Schimmoeller, T.W. Hansen, J.E.T. Andersen, S.E. Pratsinis, J.D. Grunwaldta, Journal of Molecular Catalysis A331 (2010) 40–49.
[11] T.C.O. Mac Leod, R.S. Marques, M.A. Schiavon, M.D. Assis, Applied Catalysis B: Environmental 100 (2010) 55–61.
[12] S.Y. Huang, P. Ganesan, B.N. Popov, Applied Catalysis B: Environmental 96 (2010) 224–231.
[13] M.A. Hasnat, M.S. Alam, M.H. Mahbub-ul Karim, M.A. Rashed, M. Machida, Applied Catalysis B: Environmental 107 (2011) 294–301.
[14] D.M. Dotzauer, J. Dai, L. Sun, M.L. Bruening, Nano Letters 6 (2006) 2268–2272.
[15] Y. Uozumi, Y.M.A. Yamada, T. Beppu, N. Fukuyama, M. Ueno, T. Kitamori, Journal of the American Chemical Society 128 (2006) 15994–15995.
[16] D. Wang, Y. Song, J. Wang, X. Ge, Y. Wang, A.A. Stec, H.T. Richard, Nanoscale Research Letters 4 (2009) 303–306.
[17] J.M. Campelo, D. Luna, R. Luque, J.M. Marinas, A.A. Romero, ChemSusChem 2 (2009) 18–45.
[18] S. Kidambi, M.L. Bruening, Chemistry of Materials 17 (2005) 301–307.
[19] S. Kidambi, J. Dai, J. Li, M.L. Bruening, Journal of the American Chemical Society 126 (2004) 2658–2659.
[20] D.M. Dotzauer, S. Bhattacharjee, Y. Wen, M.L. Bruening, Langmuir 25 (2009) 1865–1871.
[21] J. Macanas, L. Ouyang, M.L. Bruening, M. Munoz, J.C. Remigy, J.F. Lahitte, Catalysis Today 156 (2010) 181–186.
[22] B. Domenech, M. Munoz, D.N. Muraviev, J. Macanas, Nanoscale Research Letters 6 (2011) 406–410.
[23] M.G. Buonomenna, E. Drioli, Organic Process Research and Development 12 (2008) 982–988.
[24] M.G. Buonomenna, E. Drioli, Applied Catalysis B: Environmental 79 (2008) 35–42.
[25] G. Grigoropoulou, J.H. Clark, D.W. Hall, K. Scott, Chemical Communications 54 (2001) 7–548.
[26] J.A. Dalmon, A.C. Lopez, D. Farrusseng, N. Guilhaume, E. Iojoiu, J.C. Jalibert, S. Miachon, C. Mirodatos, A. Pantazidis, M.R. Dassonneville, Y. Schuurman, A.C. van Veen, Applied Catalysis A: General 325 (2007) 198–204.
[27] J.H. Ke, A.S. Kumar, J.W. Sue, S. Venkatesan, J.M. Zen, Journal of Molecular Catalysis A233 (2005) 111–120.
[28] S. Parra, L. Henao, E. Mielczarski, J. Mielczarski, P. Albers, E. Suvorova, J. Guindet, J. Kiwi, Langmuir 20 (2004) 5621–5629.
[29] S. Faraji, K.J. Nordheden, S.M. Stagg-Williams, Applied Catalysis B: Environmental 99 (2010) 118–126.
[30] J.F. Blanco, Q.T. Nguyen, P. Schaetzel, Journal of Membrane Science 186 (2001) 267–279.
[31] K. Miyatake, Y. Chikashige, M. Watanabe, Macromolecules 36 (2003) 9691–9693.
[32] Y.S. Kim, B. Einsla, M. Sankir, W. Harrison, B.S. Pivovar, Polymer 47 (2006) 4026–4035.
[33] M.A. Hickner, H. Ghassemi, Y.S. Kim, B.R. Einsla, J.E. McGrath, Chemical Reviews 104 (2004) 4587–4612.
[34] A. Saxena, V.K. Shahi, Journal of Membrane Science 299 (2007) 211–221.
[35] H.B. Park, B.D. Freeman, Z.B. Zhang, M. Sankir, J.E. McGrath, Angewandte Chemie International Edition 120 (2008) 6108–6113.
[36] C.D. Pina, E. Falletta, M. Rossi, Journal of Catalysis 260 (2008) 384–386.
[37] V.R. Choudhary, P.A. Chaudhari, V.S. Narkhede, Catalysis Communications (2003) 171–175.
[38] A.J. Shen, W. Shan, Y. Zhang, J. Du, H. Xu, K. fan, W. Shen, Y. Tang, Journal of Catalysis 237 (2006) 94–101.
[39] S. Alvonitis, W.T. Hanbury, T. Hodgkeiss, Desalination 85 (1992) 321–334.
[40] S. Prakash, A.M. Rajesh, V.K. Shahi, Chemical Engineering Journal 168 (2011) 108–114.
[41] B.P. Tripathi, M. Kumar, V.K. Shahi, Journal of Membrane Science 360 (2010) 90–101.
[42] Y. Yamada, Y. Fukunishi, S. Yamazaki, S. Fukuzumi, Chemical Communications 46 (2010) 7334–7336.
[43] B.D. Cullity, Elements of X-ray Diffraction, second ed., 1978.
[44] B.E. Warren, Diffraction by Imperfect Crystals, Dover Publication, New York, 1969, p. 25.

[45] A.S. Kumar, J.M. Zen, Electroanalysis 16 (2004) 242–246.
[46] P. Liu, J. Bandara, Y. Lin, D. Elgin, L.F. Allard, Y.P. Sun, Langmuir 18 (2002) 10398–10401.
[47] A.S. Kumar, J.M. Zen, Chemical Physics and Physical Chemistry 5 (2004) 1221–1227.
[48] M.S. Thompson, T.J. Meyer, Journal of the American Chemical Society 102 (1980) 2310–2312.
[49] A. Quintanilla, S.G. Rodríguez, C.M. Domínguez, S. Blasco, J.A. Casas, J.J. Rodriguez, Applied Catalysis B: Environmental 111–112 (2011) 81–89.
[50] A. Malek, K. Li, W.K. Teo, Industrial and Engineering Chemistry Research 36 (1997) 784–793.